Journal of Materials Chemistry C

Accepted Manuscript

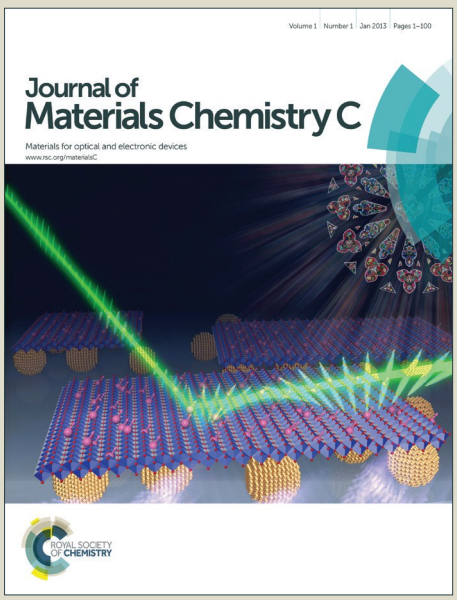

ROYAL SOCIETY OF CHEMISTRY

www.rsc.org/materialsC

Journal Name

RSCPublishing

ARTICLE

Enhanced Electro-optic Activity from the Triarylaminophenyl -Based Chromophores by introducing heteroatoms to the Donor

Cite this: DOI: 10.1039/x0xx00000x

Received 00th March 2015,
Accepted 00th March 2015

DOI: 10.1039/x0xx00000x

www.rsc.org/

Yuhui Yang [ab], Fenggang Liu [ab], Haoran Wang [ab], Shuhui Bo [a], Jialei Liu [a], Ling Qiu [a], Zhen Zhen [a], Xinhou Liu [*a]

A series of chromophores T1-T3 based on the same thiophene π-conjugation and tricyanofuran acceptor (TCF) but with different heteroatoms to the triarylaminophenyl (TAA) donors have been synthesized and systematically investigated in this paper. Density functional theory (DFT) was used to calculate the HOMO–LUMO energy gaps and first-order hyperpolarizability (β) of these chromophores. Besides, to determine the redox properties of these chromophores, cyclic voltammetry (CV) experiments were performed. After introducing the heteroatom to the benzene ring of the TAA donor, reduced energy gaps of 1.28 and 0.84 eV were obtained for chromophore T2 and T3 respectively, much lower than chromophore T1 ($\Delta E_{=}$ 1.46 eV). These chromophores showed excellent thermal stability with their decomposition temperatures all above 280℃. Besides, compared with results obtained from the chromophore (T1) without the heteroatom, these new chromophores show better intramolecular charge-transfer (ICT) absorption. Most importantly, the high molecular hyperpolarizability (β) of these chromophores can be effectively translated into large electro-optic (EO) coefficients (r_{33}) in the poled polymers. The electro-optic coefficient of poled films containing 25%wt of these new chromophores doped in amorphous polycarbonate (APC) afforded values of 16, 58 and 95 pm/V at 1310 nm for chromophores T1-T3 respectively. High r_{33} values indicated that introducing heteroatom to the benzene ring of TAA donor can efficiently improve the electron-donating ability improving the hyperpolarizability (β) and the long-chain on the benzene ring of TAA donor act as the isolation group may reduce intermolecular electrostatic interactions, thus enhancing the macroscopic EO activity. These properties, together with the good solubility, suggest the potential use of these new chromophores as advanced material devices.

1. Introduction

Development of highly efficient organic electrooptic (EO) materials has been the focal point of recent research among many organic materials research groups. This research is driven by the attractive potential of improving the efficiency of nonlinear optical (NLO) material while lowering production cost for applications including electrooptic modulation (the Pockels effect), optical rectification, and terahertz radiation generation and detection. [1-4] Over the past decade, considerable progress has been made on developing organic and polymeric electro-optic (EO) materials for applications in high-speed and broadband information technology.[5-9] One of the often encountered challenges in making highly efficient EO materials is to develop nonlinear optical (NLO) chromophores with large

hyperpolarizabilities (β) and excellent thermal stabilities.[10-12] When considering the design of dipolar π-conjugated chromophores as organic second-order nonlinear optical materials, optimization of electron donor and electron acceptor substituents is necessary to obtain maximum nonlinearity at the molecular level. Moreover, chemical, photochemical, and thermal stability in turn depend on the nature of these groups.

In general, the dipolar second-order NLO chromophore consists of a π-conjugated bridge end-capped with strong electron donor and acceptor substituents (D-π-A). Structure-property relationships that have been established indicate that large β values of the chromophores can be achieved by careful modification of the strength of donor and acceptor moieties, as well as the nature and length of the π-conjugated spacer.[13] In order to optimize molecular hyperpolarizability, much effort has been focused on the design and synthesis of optimized conjugated bridge and electron acceptor structures.[14-19] However, in the newest generation of EO chromophores, the donor units have remained relatively unchanged. Building upon this knowledge, we envisaged that a further enhancement of molecular hyperpolarizability could be achieved by introducing stronger electron donors. Unfortunately, the relative inflexibility of the structural making up of the currently available chromophore electron donor units have presented hurdles in this path for achieving durable materials with enhanced electrooptic activity, possessing a balance of all desirable qualities.

One class of NLO chromophores with a triarylamine (TAA) donor and a thiophene-bridge exhibits the highest thermal stability of all reported chromophores,[4, 20-22] which seems to be the best candidate for the active EO materials in a practical device. However, compared to their alkyl counterparts, these triarylamine (TAA) based chromophores usually exhibit reduced hyperpolarizabilities due to delocalization of the nitrogen lone pair into the two phenyl rings which do not connect with the bridge. Besides, the r_{33} values derived from aryl D-π-A chromophores remained 10-20 pm/V (at 1310 nm), which are much lower than those obtained from their alkyl D-π-A counterparts.[20, 23, 24] This may be due to the poling efficiency of these materials being strongly attenuated by large dipole-dipole and π-π stacking interactions, and charge transporting between their triarylamino moieties under high poling electric fields. [18, 25-27]This encouraged us to modify TAA based chromophores to improve their r_{33} values and thus overcome their drawbacks while maintaining high thermal stability.

In this paper, we have designed and synthesized three D-π-A chromophores (T1-T3) in Chart 1 for conducting a systematic study of their structure/property relationships. All designed model chromophores have the same thiophene-bridge and strong electron acceptor TCF. They showed great solubility in common organic solvents, good compatibility with polymers, and large EO activity in the poled films. ^{1}H-NMR and ^{13}C-NMR analysis were carried out to demonstrate the preparation of these chromophores. Thermal stability, photophysical properties, DFT calculations and EO activities of these chromophores were systematically studied and were compared with the unmodified TAA chromophore (Chart 1). Our results reveal that by introducing the heteroatom to the benzene ring of TAA donor can dramatically affect their nonlinear optical properties. In a properly designed system, significant enhancement in the hyperpolarizability of TAA based NLO chromophores can be achieved compared to unsubstituted TAA chromophore.

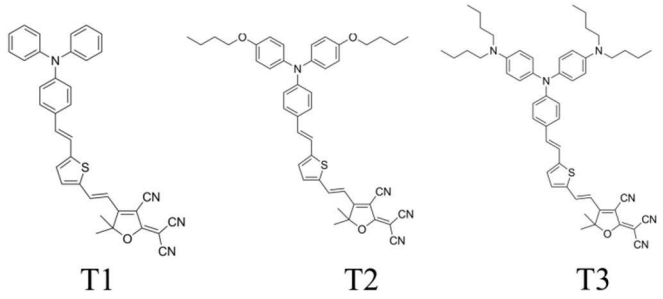

Chart 1 The structures of chromophore T1-T3

2. Results and discussion

2.1 Synthesis and characterization of chromophores

Synthesis of T1, T2 and T3 chromophores were depicted in scheme 1, scheme 2 and scheme 3, respectively. Unmodified chromophore T1 was synthsised according to the literature.[20] The modified chromophore T2 and T3 were prepared according to different strategies. Chromophore T2 was obtained in six steps starting from the commercially available Iodophenol (Scheme 2). The alkylation of 4-iodophenol with bromobutane in the presence of K_2CO_3 gave 1b, and subsequent conversion to 2b according to the modified Ullmann Condensation reaction[28] that was in turn converted to give 3b by the Vielsmier reaction.[29] The aldehyde 3b was condensed with 2-thienyltriphenylphosphonate bromide by Wittig condensation to gain 4b. As expected, after introduction of the thiophene bridge by Wittig condensation, treatment of compound 4b with n-BuLi and DMF gave an aldehyde 5b. The target chromophore T2 was obtained via Knoevenagel condensation reaction of the aldehyde 5b with acceptor TCF in the presence of a catalytic amount of triethylamine.

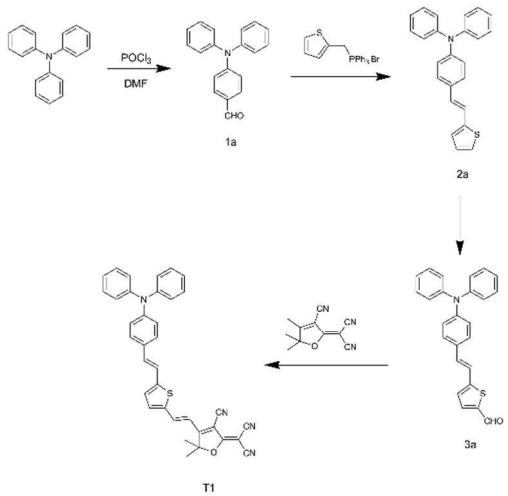

Scheme 1 Synthetic scheme for chromophore T1

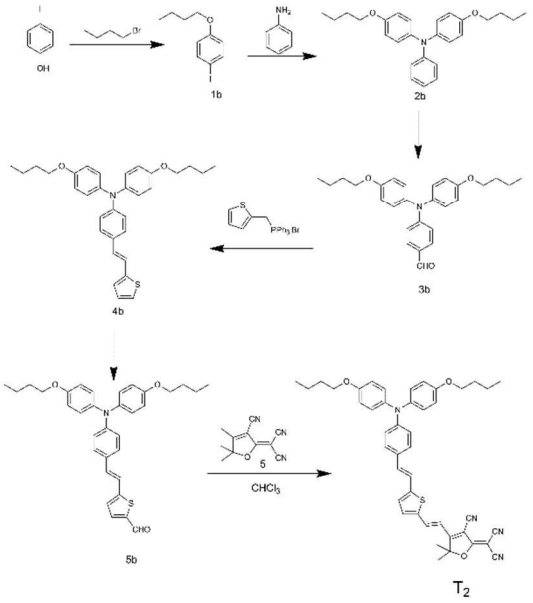

Scheme 2 Synthetic scheme for chromophore T2

Chromophore T3 was obtained by six steps in a different way (Scheme 3). The crucial reaction involves the synthesis of the donor group of compound 3c. To obtain compound 3c, we use two different methods. It was starting from commercially available triphenylamine with Vielsmier reaction for the preparation of triphenylamine aldehyde and subsequent treatment it with potassium iodide and potassium iodate in acetic acid led to intermediates 1d yields of 91 %. The compounds **3c** were synthesized by the Ullmann reaction from triphenylamine aldehyde iodide using the powerful catalytic system about the combination of CuI and 2-(2,6-dimethylphenylamino)- 2-oxoacetic acid (DMPAO). In order to improve the yields, we also found another useful procedure. Treatment N, N - butyl aniline with potassium iodide and potassium iodate in acetic acid led to intermediates 1c yields of

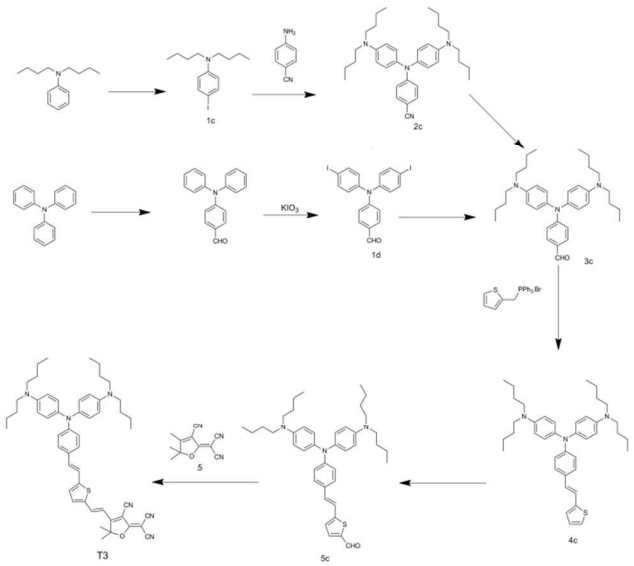

Scheme 3 Synthetic scheme for chromophore T3

88 % and subsequent conversion to 2c according to the modified Ullmann Condensation reaction. The reduction with DIBAL-H followed by acid hydrolysis converts the nitrile group on 2c into the corresponding aldehyde 3c with 86% yield. The aldehyde 3c was condensed with 2-thienyltriphenylphosphonate bromide by Witting condensation to gain 4c. As expected, after introduction of the thiophene bridge by Wittig condensation, treatment of compound 4b with n-BuLi and DMF gave an aldehyde 5c. The target chromophore T3 was obtained via Knoevenagel condensation reaction of the aldehyde 5c with acceptor TCF in the presence of a catalytic amount of triethylamine**.**

All of the chromophores were fully characterized by ^{1}H-NMR, ^{13}C-NMR, and mass spectroscopy. These chromophores possess good solubility in common organic solvents, such as dichloromethane, chloromethane and acetone.

2.2 Thermal analysis.

NLO chromophores must be thermally stable enough to withstand encountered high temperatures (>200℃) in electric field poling and subsequent processing of chromophore/polymer materials. Thermal properties of these chromophores were measured by Thermogravimetric Analysis (TGA). The decomposition temperature (T_d) of chromophores T1-T3 is all above 280 °C. All of these chromophores showed excellent stability. It should be pointed out that the stronger donor strength provided by adding the buthoxy groups and dibutylamine did not compromise the thermal stability of the resulting chromophores. The T_d of these chromophores was high enough for the application in EO device preparation.

2.3 Optical properties

In order to reveal the effect of heteroatom on the intromolecular charge transfer (ICT) of dipolar chromophores, UV-Vis absorption spectra of three chromophores ($c=1\times10^{-5}$ mol/L) were measured in a series of aprotic solvents with different polarity so that the solvatochromic behavior of these chromophores could be investigated to explore the polarity of chromphores in a wide range of dielectric environments (Figure1). The spectrum data are summarized in Table 1. The synthesized chromophores exhibited a similar $\pi\rightarrow\pi^{*}$ intramolecular charge-transfer (ICT) absorption band in the visible region. T1 shows a maximum absorption (λ_{max}) of 621nm. With two additional butoxy group on the donor, the λ_{max} of T2 red shifted by 44 nm to 665 nm. With two additional butylamine groups on the donor, the λ_{max} of T3 further red-shifted to 730 nm. This result clearly shows that the butoxy groups and butylamine groups provide extra donating strength to the donor part, shifting the ICT absorption band of the chromophore to the lower energy. As shown in Figure 1, peak wavelength of T1, T2 and T3 showed a bathochromic shift of 44, 48 and 72 nm from dioxane to chloroform respectively. Chromophore T3 displayed the larger solvatochromism compared with the T1 and T2. The resulting spectrum data confirmed that the chromophore with butylamine groups on the donor was more easily polarizable than the chromophore with

the butoxy groups on the donor. These analyses implied that the butylamine groups on the donor improved the electron-donating

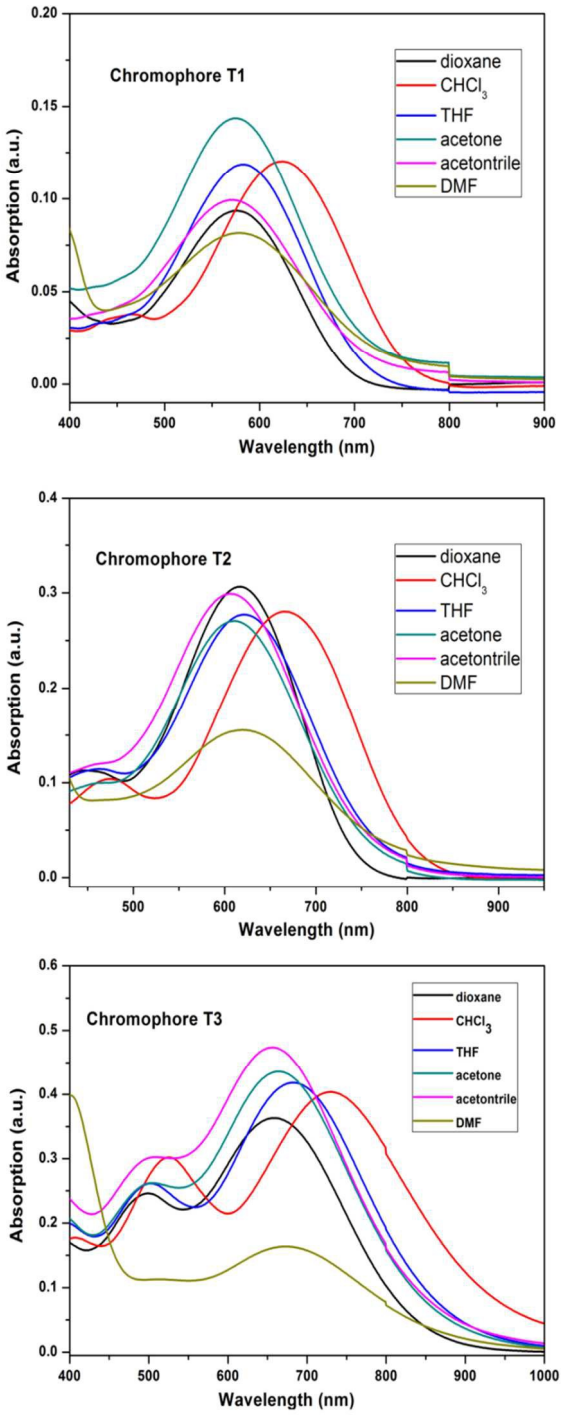

Figure 1 UV-Vis absorption spectra in different solvents of chromophore T1-T3(c = 1×10^{-5} mol

capability and increased the polarizability.

Traditional chromophores were easy to aggregate, which were beneficial for self-assembly. However, it was unfavorable for the NLO application, because these chromophores were easy to form the antiparallel aggregation. This phenomenon can

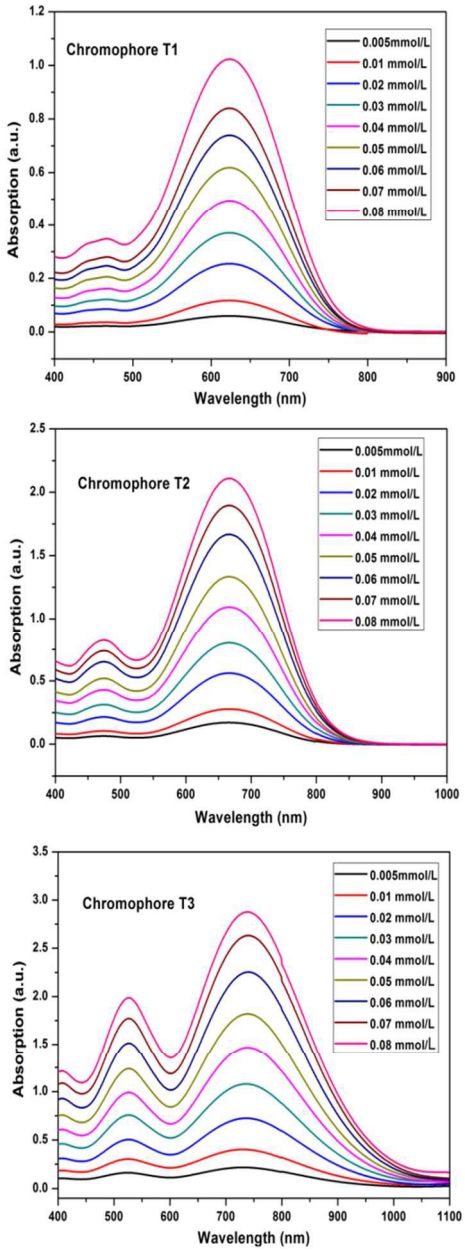

Figure 2 UV-Vis absorption spectra of different concentrations of chromophores

be demonstrated by absorption intensity, wavelength and shape of absorption band in UV-vis spectra. To study the effect of heteroatom on attenuating chromophore aggregation, the absorption of the chromophore was measured in $CHCl_3$ at different concentration (range from 0.005 mM to 0.08 mM). As Figure 2 showed, the λ_{max} of the chromophore at different concentration. As the concentration rose, no obvious blue-shift or red-shift was found. Even at high concentration, no obvious characteristic absorption band of aggregation was observed.

Table1 . Summary of Thermal and Optical Properties and EO Coefficients of Chromophores T1-T3

Chronmophore	T_d[a] (℃)	λ^b_{max}(nm)	λ^c_{max}(nm)	$\Delta\lambda$[d] (nm)	r^e_{33}(pm/V)
T1	301	621	577	44	16
T2	310	665	617	48	58
T3	289	730	658	72	95

[a] T_d was determined by an onset point, and measured by TGA under nitrogen at a heating rate of 10 ℃ /min.

[b] λ_{max} was measured in $CHCl_3$.

[c] λ_{max} was measured in dioxane.

[d] $\Delta\lambda=\lambda^b_{max}-\lambda^c_{max}$

[e] r_{33} values were measured at the wavelength of 1310 nm.

2.4 Theoritical calculations

In order to model the ground state molecular geometries, the HOMO-LUMO energy gaps and β values of these chromophores were calculated. The DFT calculations were carried out at the hybrid B3LYP level by employing the split valence 6-311 g (d, p) basis set. [30-32] The data obtained from DFT calculations are summarized in Table 2.

The frontier molecular orbitals are often used to characterize the chemical reactivity and kinetic stability of a molecule and to obtain qualitative information about the optical and electrical properties of molecules.[32, 33, 34] Besides, the HOMO-LUMO Energy gap is also used to understand the charge transfer interaction occurring in a chromophore molecule. [34-36] In the case of these chromophores, Figure 3 represents the frontier molecular orbitals of chromophores T1, T2 and T3. According to the Figure 3, it is clear that the electronic distribution of the HOMO is delocalized over the thiophene linkage and benzene ring, whereas the LUMO is mainly constituted by the acceptor moieties.[34]

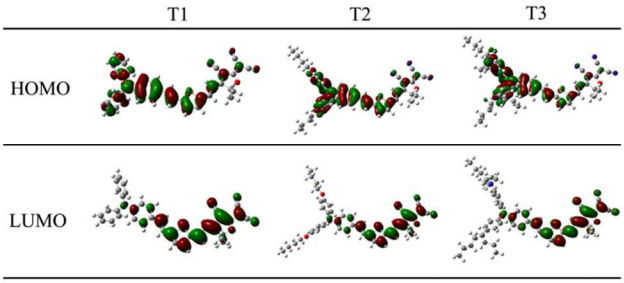

Figure 3 The frontier molecular orbitals of chromophores T1-T3

The HOMO and LUMO energy were calculated by DFT calculations as shown in Figure 3 and Table 2. For the chromophore T3, the new donor structure narrows the energy gap between the HOMO and LUMO energy with ΔE values of 1.68 eV. The DE value of T2 is 1.87 eV. By contrast, the ΔE value of T1 is 2.20 eV. As the data showed, the LUMO energy of the three chromophores has no obvious difference. However, the HOMO energy varied widely. The HOMO energy of chromophore T3 is 0.52 eV larger than that of T1 (−4.97 eV vs. −5.49 eV) and is 0.26 eV larger than that of T2 (−4.97 eV vs. −5.23 eV). This may resulted from the fact that the heteroatom on donor structure influences the HOMO energy to a greater extent than the LUMO energy. The HOMO–LUMO gaps of chromphore T3 (1.68 eV) is lowest and T1 (2.20 eV) is the largest. This result indicates that T3 may exhibit better ICT and NLO property than T2 and T1. As repoted[34], the optical gap is lower, the charge-transfer (ICT) ability is greater and thus improve the nonlinearity. Chromophore T3 showed a lower optical gap, so it indicated that T3 may exhibit better ICT and NLO property than the other two chromophores.

Table2. Data from DFT calculations

Chromophores	E_{HOMO}/eV	E_{LUMO}/eV	Δ E[a]/eV	Δ E[b]/eV	βmax[c]/10^{-30}esu
T1	-5.49	-3.29	2.20	1.46	1162
T2	-5.23	-3.36	1.87	1.28	1642
T3	-4.97	-3.29	1.68	0.84	2428

Δ E = E_{LUMO} - E_{HOMO},

[a] Results was calculated by DFT

[b] Results was from cyclic voltammetry experiment

[c] β values were calculated using gussian03at B3LYP/6-311 g** (d, p) level and the direction of the maximum value is directed along the charge transfer axis of the chromophores.

Further, the theoretical microscopic Zero-frequency (static) molecular first hyperpolarizability β was calculated by Gaussian 03. As the reference reported earlier, the β values have been calculated at the 6-311 g** (d, p) level in vacuum. [37] From this, the scalar quantity of β can be computed from the x, y, and z components according to the following equation:

$$\beta = (\beta_x^2 + \beta_y^2 + \beta_z^2)^{1/2} \quad (1)$$

Where $\beta_i = \beta_{iii} + \frac{1}{3}\sum_{i\neq j}(\beta_{ijj} + \beta_{jij} + \beta_{jji}), \quad i, j \in (x, y, z)$

Due to the stronger electron-donating ability and better conjugated system (Figure 4), chromophore T3 showed much larger β value than the other two chromophores, while the chromophore T1 exhibited the smallest β value (1162×10^{-30} esu). This result is well corresponded with the conclusion of UV-Vis spectra analysis.

2.5 Electrochemical properties

To determine the redox properties of these chromophores, cyclic voltammetry (CV) experiments were performed on BAS CV-50W voltammetric analyzer using a conventional three-electrode cell with Pt metal as the working electrode, a Pt gauze as the counter-electrode, and $Ag/AgNO_3$ as the reference electrode at a scan rate of 50 mV s^{-1}. 0.1 M Tetrabutylammonium hexafluorophosphate (TBAPF) in acetonitrile is the electrolyte. As shown in the Figure 5, chromophores T1, T2 and T3 all exhibited one quasi reversible

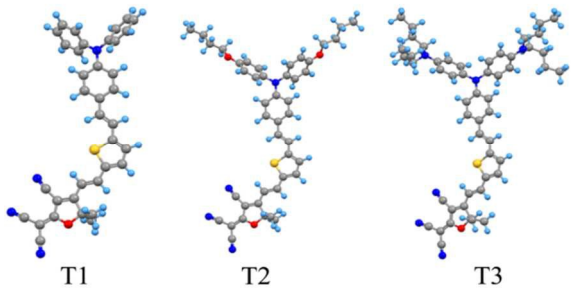

Figure 4 The optimized structure of chromophore

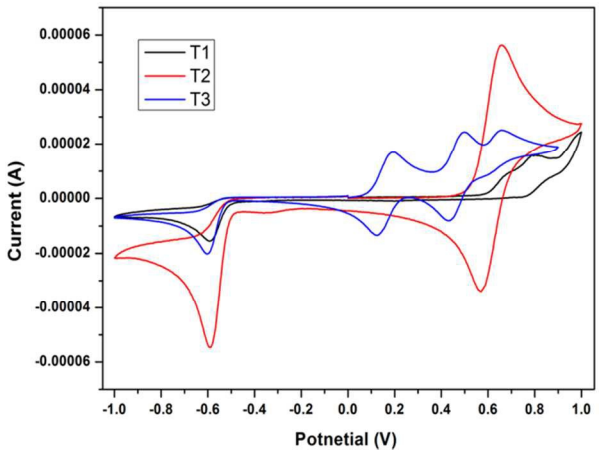

Figure 5 Cyclic voltammograms of chromophore T1-T3

oxidative wave with a half-wave potential, $E_{1/2}= 0.5(E_{ox} + E_{red})$, at about 0.75, 0.62 and 0.15 V respectively. Chromophore T3 showed two oxidation waves, the first one is a reversible wave with half-wave potentials at about 0.15 V corresponding to the donor group. Meanwhile, these chromophores had an irreversible reduction wave corresponding to the acceptor moieties at E_{red} =-0.71, -0.66 and -0.69 V (vs. $Ag/AgNO_3$). It showed an energy gap (ΔE) value of 1.46, 1.28 and 0.84 eV for chromophores T1, T2 and T3 respectively. The HOMO and LUMO levels of these new chromophores were calculated from their corresponding oxidation and reduction potentials. The HOMO levels of T1, T2 and T3 were estimated to be -5.15, -5.02 and -4.55 eV respectively. In the meantime, the corresponding LUMO level of T1-T3 only showed slight changes at -3.69, -3.74 and -3.71 eV, respectively. This result corresponded with the conclusion of UV-Vis spectra analysis and the DFT results.

2.6 Electric field poling and EO property measurements.

For studying EO property derived from these chromophores, a series of guest-host polymers were generated by formulating the chromophores into amorphous polycarbonate (APC) using dibromomethane as solvent. The resulting solutions were filtered through a 0.2-μm PTFE filter and spin-coated onto indium tin oxide (ITO) glass substrates. Films of doped polymers were baked in a vacuum oven at 80 ℃ overnight to ensure the removal of the residual solvent. The corona poling process was carried out at a temperature of 10 ℃ above the glass transition temperature (T_g) of the polymer. The r_{33} values were measured using the Teng-Man simple reflection technique at the wavelength of 1310 nm using a carefully selected thin ITO electrode with low reflectivity and good transparency in order to minimize the contribution from multiple reflections. [38]

For dipolar chromophores in an electric poling field, the electro-optic coefficient (r_{33}) in the direction of the applied field is related to the molecular first hyperpolarizability and was described as follows:

$$r_{33} =2N f(\omega) \beta<\cos^3\theta>/n^4 \quad (2)$$

Where r_{33} is the EO coefficient of the poled polymer, N represents the aligned chromophore number density and f(ω) denotes the Lorentz-Onsager local field factors. The term $<\cos^3\theta>$ is the orientationally averaged acentric order parameter characterizing the degree of noncentrosymmetric alignment of the chromophore in the material and n represents the refractive index.[39] Before poling, there is no EO activity in the EO material and the chromophores in material are thermal randomization. Electrical field induced poling was proceeded to induce the acentric ordering of chromophores. Realization of large electro-optic activity for dipolar organic chromophore-containing materials requires the simultaneous optimization of chromophore first hyperpolarizability (β), acentric order $<\cos^3\theta>$, and number density (N). At low concentration, the electro-optic activity increased with chromophore density, dipole moment and the strength of the electric poling field. However, when the concentrations of chromophores increased to a certain extent, the N and $<\cos^3\theta>$ are no longer independent factors. Then

$$<\cos^3\theta>= (\mu F/5kT)[1-L^2(W/kT)] \quad (3)$$

Where k is the Boltzmann constant and T is the Kelvin (poling) temperature. $F =[f(0)E_P]$ where E_p is the electric poling field. L is the Langevin function, which is a function of W/kT, the ratio of the intermolecular electrostatic energy (W) to the thermal energy (kT). L is related to electrostatic interactions between molecules. So when the intermolecular electrostatic interactions are neglected, the electro-optic coefficient (r_{33}) should increase linearly with chromophore density, dipole moment, first hyperpolarizability and the strength of the electric poling field.

The r_{33} values of films containing chromophores T1 (fillm-A), T2 (film-B), T3 (film-C) were measured at different loading densities, as shown in table 3 and Figure 6, For chromophore T1, the r_{33} values were gradually improved from 7 pm V^{-1} (10 wt%) to 16 pm V^{-1} (25 wt%), as the concentration of chromophores increased, the similar trend of enhancement was also observed for chromophore T2, whose r_{33} values increased from the 19 pm V^{-1} (10 wt%) to 58 pm V^{-1} (25 wt%). Chromophoe T3 gained the r_{33} value from 28 pm V^{-1} (10 wt%) to 95 pm V^{-1} (25 wt%). When the loading density increasing from 25 wt % to 30 wt %, the film-A with the loading 30 wt % of T1 presents an obvious phase separation and film-B, film-C displayed a downward trend.

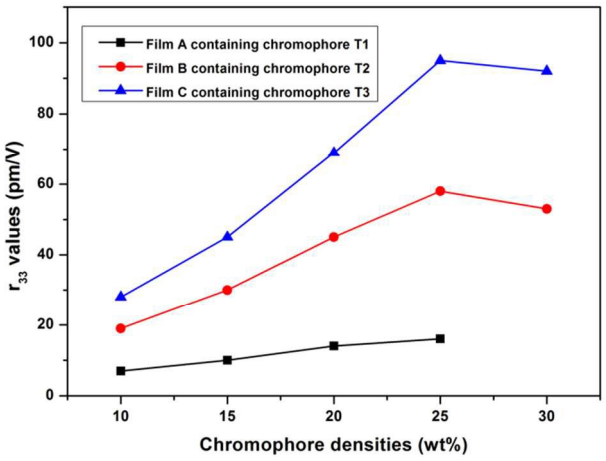

Figure 6 EO coefficients of NLO thin films as a function of chromophore loading densities

Through the outcome above, we can obviously see that the film- B containing chromophore T2 have nearly 4 times higher r_{33} value and film - C containing chromophore T3 have nearly 6 times higher r_{33} values than the film-A containing the chromophore T1, which illustrating that the increased donor strength of the chromophores significantly increase their macroscopic EO activities. This result can be explained as follows: When the concentration of chromophore in APC is low, the intermolecular dipolar interactions are relatively weak. The film-C/APC achieved the largest r_{33} value probably due to its largest β and good polarizability. With relatively low β, the r_{33} value of film-B/APC was smaller than that of film-C/APC. The drop in EO activity from film-B/APC to film-A/APC is mainly associated with the lowest β of chromophore A in the polar polymer matrix and the inefficient poling, because of its lower polarizability than the other two chromophores.

As the chromophore loading densities increased, the effect of inter-chromophore dipole–dipole interaction is becoming stronger. Chromophore T2 with two butoxy groups on the aromatic amino donor was designed to optimize the shape of

Table 3 Summary of EO Coefficients of Chromophores T1-T3 at different densities

	[a]r_{33} (pm/V)		
Wt%	T1	T2	T3
10	7	19	28
15	10	30	45
20	14	45	69
25	16	58	95
30	--	53	92

[a] r_{33} values were measured at the wavelength of 1310nm.

chromophore. The butoxy group was also used to increase the solubility of the chromophore. In a similar way, chromophore T3 with the butylamide group also can control the shape of the chromophore and increased solublity as well. As reported,[40] the introduction of some isolation groups to the chromophore moieties to further control the shape of the chromophore could be an efficient approach to minimize interactions between the chromophores. So when the chromophore loading increased, the introduction of groups attached to the donor system can make inter-chromophore electrostatic interactions less favorable and thus increased the macroscopic EO activity. So film - C presented the largest r_{33} values and film A containing T1 showed the smallest r_{33} values. This corresponded well with the results of the solvatochromism study, DFT calculations and redox properties of chromophores.

3. Experimental

3.1 Materials and instrumentation

1H NMR spectra were determined by an Advance Bruker 400(400 MHZ) NMR spectrometer (tetramethylsilane as internal reference). The MS spectra were obtained on MALDI-TOF-(Matrix Assisted Laser Desorption/Ionization of Flight) on BIFLEXIII(Broker Inc.) spectrometer. The UV-Vis spectra were performed on Cary 5000 photo spectrometer. The TGA was determined by TA5000-2950TGA (TA Co) with a heating rate of 10℃/ min under the protection of nitrogen. Cyclic voltammetry (CV) experiments were performed were performed on BAS CV-50W voltammetric analyzer using a conventional three-electrode cell with Pt metal as the working electrode, a Pt gauze as the counter-electrode, and $Ag/AgNO_3$ as the reference electrode at a scan rate of 50 mV s^{-1}. 0.1 M Tetrabutylammonium hexafluorophosphate (TBAPF) in acetonitrile is the electrolyte. The ferrocene/ferrocenium (Fc/Fc+) couple was used as an internal reference. The elemental analysis was performed on a Flash EA 1112 elemental analyzer. All chemicals, commercially available, are used without further purification unless stated. The DMF, POCl3 and THF were freshly distilled prior to its use. The 2-dicyanomethylene-3-cyano-4-methyl-2,5-dihydrofuran (TCF) acceptor was prepared according to the literature.[41]

3.2 Synthesis.

3.2.1 Compound 1a was synthesized according to the literature.[20].

3.2.2 Synthesis of conpound 2a

Under N2, to a mixture of compound 1a (1.37 g, 5 mmol) and 2-thienyl triphenylphosphonate bromide (2.64 g, 6 mmol) in dry THF (20 mL) at room temperature, NaH (1.20 g, 0.05 mol) was added. The mixture turned yellow and was stirred at room temperature for 24 h. Saturated NH_4Cl was added and the resulting mixture was extracted with EtOAc (20/×3 mL). The combined extracts were washed with water and dried over MgSO4. After filtration and removal of the solvent under vacuum, the residue was purified by column chromatography on silica gel (hexane/acetone, v/v, 10/1) to obtain a yellow solid (1.22 g, 69%).

^{1}H NMR (400 MHz, $CDCl_3$) δ 7.32 (d, J = 8.5 Hz, 2H), 7.25 – 7.23 (m, 4H), 7.16-7.23 (m, 5H), 7.13 – 7.08 (m, 5H), 7.02-7.08 (m, 2H), 6.87 (d, J = 16.2 Hz, 1H).

^{13}C NMR (100 MHz, $CDCl_3$): δ 120.18, 123.06, 123.52, 123.84, 124.52, 125.48, 127.14, 127.55, 127.92, 129.25, 131.06, 143.27, 147.20, 147.52.

MALDI-TOF: m/z calcd for $C_{24}H_{19}NS$: 353.48 $[M]^+$; found: 353.57.

3.2.3 Synthesis of conpound 3a

To a solution of compound 2a (1.06 g, 3.00 mmol) in dry THF (20 mL) a 2.4 M solution of n-BuLi in hexane (1.9 mL, 4.50 mmol) was added dropwise at −78 ℃ under N2. After this mixture was stirred at this temperature for 1 h, dry DMF (0.28 mL, 3.60 mmol) was introduced. The resulting solution was stirred for another 1h at −78 ℃ and then allowed to warm up to room temperature. The reaction was quenched by water. THF was removed by evaporation. The residue was extracted using CH_2Cl_2 (3×30 mL). The organic layer was dried by $MgSO_4$ and concentrated in vacuo. The residue was purified by column chromatography on silica gel (hexane/acetone, v/v, 10/1) to obtain a red solid (0.94g, 82%).

^{1}H NMR (400 MHz, $CDCl_3$) δ 9.82 (s, 1H), 7.63 (d, J = 3.9 Hz, 1H), 7.34 (d, J = 8.5 Hz, 2H), 7.30 – 7.24 (m, 4H), 7.11 (d, J = 7.9 Hz, 4H), 7.10 – 7.04 (m, 5H), 7.02 (d, J = 8.6 Hz, 2H).

^{13}C NMR (100 MHz, $CDCl_3$) δ 177.93, 148.86, 144.33, 142.98, 136.86, 132.86, 128.31, 125.02, 123.66, 121.56, 120.74, 119.35, 118.44, 114.58, 114.55.
MALDI-TOF: m/z calcd for $C_{25}H_{19}NOS$: 381.49 $[M]^+$; found: 381.47.

3.2.4 Synthesis of chromophore T1

A mixture of aldehydic bridge 5 (0.38 g, 1.00 mmol) and acceptor 6 (0.22 g, 1.10 mmol) in chloroform (30 mL) was stirred at 62℃ for 4 h in the presence of a catalytic amount of triethylamine. After removal of the solvent, the residue was purified by column chromatography on silica gel (hexane/acetone, v/v, 5:1). A dark solid was obtained (0.21 g, 38%).
^{1}H NMR (400 MHz, $CDCl_3$) δ 7.78 (d, J = 15.7 Hz, 1H), 7.41 – 7.33 (m, 3H), 7.29 (dd, J = 14.6, 6.8 Hz, 5H), 7.10 (dd, J = 24.2, 11.3 Hz, 8H), 7.03 (d, J = 8.0 Hz, 2H), 6.61 (d, J = 15.7 Hz, 1H), 1.76 (s, 6H).
^{13}C NMR (100 MHz, $CDCl_3$) δ 171.24, 168.56, 148.52, 144.68, 142.78, 134.87, 133.74, 132.62, 129.32, 125.17, 123.63, 123.29, 120.95, 119.46, 117.91, 114.11, 108.13, 107.58, 106.83, 106.40, 92.72, 25.28, 22.19.
MALDI-TOF: m/z calcd for $C_{36}H_{26}N_4OS$: 562.68 $[M]^+$; found: 562.49.
Anal. calcd (%) for $C_{36}H_{26}N_4OS$: C, 76.84; H, 4.66; N, 9.96; found: C, 76.91; H, 4.62; N, 10.01.

3.2.5 Synthesis of compound 1b

To a stirred mixture of 4-iodophenol (12.25 g, 0.055 mol), 1-Bromobutane (8.22 g, 0.06 mol), and DMF (100 mL) under argon was added K_2CO_3 (13.80 g, 0.10 mol). The reaction mixture was refluxed for 24 h and cooled to room temperature. The resulting mixture was filtered, and then most solvent of the filtrate was evaporated. The obtained oil was dissolved in chloroform, washed with water, dried over $MgSO_4$, evaporated, and purified with column chromatography on silica gel (hexane/acetone, v/v, 10:1) to yield a colorless oil (13.05 g , 86%).
^{1}H NMR (400 MHz, $CDCl_3$) δ 7.52 (d, J = 8.3 Hz, 2H), 6.65 (d, J = 8.4 Hz, 2H), 3.89 (t, J = 6.5 Hz, 2H), 1.81 – 1.67 (m, 2H), 1.47 (dd, J = 13.4, 6.2 Hz,2H), 1.02 – 0.91 (m, 3H).
^{13}C NMR (100 MHz, CDCl3) δ 158.96, 138.07, 116.88, 82.37, 67.72, 31.15, 19.17, 13.81.
MALDI-TOF: m/z calcd for $C_{10}H_{13}OI$: 276.11 $[M]^+$; found: 276.16.

3.2.6 Synthesis of compound 2b

The mixture of 1b (8.28 g, 0.03mol), phenylamine (1.25 g, 0.013 mmol), CuCl (0.108 g, 0. 001 mmol), phenathroline (0.21 g, 0.001 mmol), KOH (13.2 g, 0.24 mol), and toluene (70 mL) was refluxed for 24 h. After cooling, the resulting mixture was poured into plenty of stirred water and extracted with chloroform. The obtained organic phase was washed several times with water, dried over magnesium sulfate, evaporated, and purified with column chromatography on silica gel (hexane/acetone, v/v, 8:1) to yield yellowish oil. (3.08 g , 61%).
^{1}H NMR (400 MHz, $CDCl_3$) δ 7.15 (d, J = 7.6 Hz, 2H), 7.02 (d, J = 8.1 Hz, 2H), 6.93 (d, J = 7.6 Hz, 2H), 6.82 (m, 5H), 3.92 (m, 2H), 1.81 – 1.70 (m, 2H), 1.55 – 1.43 (m, 2H), 0.97 (m, 3H).
^{13}C NMR (100 MHz, $CDCl_3$) δ 155.36, 148.92, 141.06, 128.95, 126.46, 120.91, 120.50, 67.97, 31.45, 19.36, 13.96.
MALDI-TOF: m/z calcd for $C_{26}H_{31}NO_2$: 389.53 $[M]^+$; found: 389.71.

3.2.7 Synthesis of compound 3b

Phosphorous oxychloride (0.7 mL, 0.007 mol) was added dropwise to a stirred DMF (1.2 mL, 0.014 mol) at 0 °C. The mixture was stirred for 1 h at 0 °C and additionally stirred at room temperature for 1 h. After the addition of compound 2b (2.92 g, 0.007mol) solution in dichloroethane (20 mL), the mixture was stirred at 90 °C for 2 h. After cooling, the solution was poured into cold water. The resulting mixture was neutralized to pH 7 with 2 M NaOH aqueous solution and extracted with chloroform. The extract was washed with plenty of brine and water, successively. The organic extracts were dried over $MgSO_4$, evaporated, and purified with column chromatography on silica gel (hexane/acetone, v/v, 10:1) to yield yellowish oil. (2.60 g , 89%).
^{1}H NMR (400 MHz, $CDCl_3$) δ 9.74 (s, 1H), 7.62 (d, J = 8.2 Hz, 2H), 7.11 (d, J = 8.3 Hz, 4H), 6.86 (m, 6H), 3.95 (m, 4H), 1.76 (m, 4H), 1.56 – 1.42 (m, 4H), 0.98 (m, 6H).
^{13}C NMR (100 MHz, $CDCl_3$) δ 190.25, 156.97, 154.16, 138.62, 131.43, 128.06, 127.70, 116.70, 67.96, 31.35, 19.28, 13.88.
MALDI-TOF: m/z calcd for $C_{27}H_{31}NO_3$: 417.54 $[M]^+$; found: 417.56.

3.2.8 Synthesis of compound 4b

In a similar manner described above, compound 4b was synthesized from 3b as yellowish oil (72%).
^{1}H NMR (400 MHz, $CDCl_3$) δ 7.25 (d, J = 8.5Hz, 2H), 7.11 (d, J = 4.7 Hz, 1H), 7.03 (d, J = 7.7 Hz, 6H), 6.99 – 6.95 (m, 1H), 6.87 (d, J = 8.4 Hz, 3H), 6.81 (d, J = 8.5 Hz, 4H), 6.55 (d, J = 11.9 Hz, 1H), 6.45 (d, J = 11.9 Hz, 1H), 3.92 (m, 4H), 1.81 – 1.70 (m, 4H), 1.49 (m, 4H), 0.96 (m, 8H).
^{13}C NMR (100 MHz, $CDCl_3$) δ 151.40, 144.19, 139.32, 136.32, 124.83, 124.04, 123.19, 122.73, 122.39, 120.70, 119.17, 116.10, 114.89, 63.76, 27.18, 14.90, 9.52.
MALDI-TOF: m/z calcd for $C_{32}H_{35}NO_2S$: 497.69 $[M]^+$; found: 497.57.

3.2.9 Synthesis of compound 5b

In a similar manner described above, compound 5b was synthesized from 4b as red oil (84%).
^{1}H NMR (400 MHz, $CDCl_3$) δ 9.81 (s, 1H), 7.62 (d, J = 3.8 Hz, 1H), 7.28 (t, J = 5.6 Hz, 2H), 7.11 – 6.99 (m, 6H), 6.85 (dd, J = 12.8, 8.6 Hz, 7H), 3.94 (m, 4H), 1.82 – 1.71 (m, 4H), 1.55 – 1.43 (m, 4H), 1.03 – 0.94 (m, 4H).
^{13}C NMR (100 MHz, $CDCl_3$) δ 177.87, 151.78, 149.31, 145.33, 136.50, 135.78, 132.88, 128.74, 123.56, 123.20, 122.77, 121.12, 115.26, 113.40, 111.20, 63.76, 52.84, 27.14, 14.97, 9.50.
MALDI-TOF: m/z calcd for $C_{33}H_{35}NO_3S$: 525.70 $[M]^+$; found: 525.83.

3.2.10 Synthesis of compound chromophore T2

In a similar manner described above, chromophore T2 was synthesized from 5b as dark solid (48%).
^{1}H NMR (400 MHz, Acetone) δ 8.15 (d, J = 15.8 Hz, 1H), 7.68 (d, J = 3.6 Hz, 1H), 7.47 (d, J = 8.5 Hz, 2H), 7.36 – 7.18 (m, 3H), 7.10 (d, J = 8.6 Hz, 4H), 6.94 (d, J = 8.6 Hz, 4H), 6.83 (m, 3H), 4.00 (m, 4H), 1.89 (m, 4H), 1.73 (s, 6H), 1.50 (m, 4H), 0.98 (m, 6H).
^{13}C NMR (100 MHz, Acetone) δ 180.24, 172.27, 172.07, 169.91, 152.16, 148.19, 145.58, 135.56, 135.40, 134.15, 133.15, 128.89, 123.89, 123.47, 123.38, 123.08, 114.52, 113.61, 111.24, 108.44, 107.98, 107.33, 107.14, 106.63, 106.48, 105.03, 100.14, 96.46, 93.84, 93.34, 27.00, 21.12, 18.89, 14.74, 9.22, 8.91.

MALDI-TOF: m/z calcd for $C_{44}H_{42}N_4O_3S$:706.89 $[M]^+$; found: 706.72.

Anal. calcd (%) for $C_{44}H_{42}N_4O_3S$: C, 74.76; H, 5.99; N, 7.93; found: C, 74.87; H, 5.94; N, 7.97.

3.2.11 Compound 1d was synthesized according to literitre.[42]

^{1}H NMR (400 MHz, $CDCl_3$) δ 9.85 (s, 1H), 7.71 (d, *J* = 8.6 Hz, 2H), 7.63 (d, *J* = 8.6 Hz, 4H), 7.05 (d, *J* = 8.6 Hz, 2H), 6.89 (d, *J* = 8.6 Hz, 4H).

^{13}C NMR (100 MHz, $CDCl_3$) δ 190.37, 152.21, 145.73, 138.88, 131.36, 130.36, 127.63, 120.78.

3.2.12 Synthesis of compound 1c

To the mixture of glacial acetic acid (50 mL) and water (10 mL), concentrated sulfuric acid (1.5 mL) was added dropwise, and then added N, N-dibutylaniline (10.3 g, 0.05 mol), iodine (5.2 g, 0.02 mol) and sodium periodate (2.5 g, 0.011 mol). The mixture maintained at 40 ℃ for 8 hours then poured in saturated solution of sodium bicarbonate (200 mL) and extracted with ethyl acetate (100 mL), and the organic layer was separated and washed 3 times with water, dried over anhydrous magnesium sulfate, and purified with column chromatography on silica gel (hexane/acetone, v/v, 50:1) to yield a yellowish liquid. (14.3g, 86%).

^{1}H NMR (400 MHz, $CDCl_3$) δ 7.40 (d, *J* = 8.0 Hz, 2H), 6.40 (d, *J* = 8.0 Hz, 2H), 3.21 (m, 4H), 1.59 – 1.45 (m, 4H), 1.39 – 1.25 (m, 4H), 0.94 (m, 6H).

^{13}C NMR (100 MHz, $CDCl_3$) δ 147.73, 137.59, 114.21, 50.70, 29.12, 20.29, 13.95.

MALDI-TOF: m/z calcd for $C_{14}H_{22}NI$: 331.24 $[M]^+$; found: 331.43.

3.2.13 synthesis of compound 2c

The mixture of 1c (9.93 g, 0.03mol), 4-Aminobenzonitrile (1.53 g, 0.013 mmol), CuCl (0.108 g, 0. 001 mmol), phenathroline (0.21 g, 0.001 mmol), KOH (13.2 g, 0.24 mol), and toluene (70 mL) was refluxed for 24 h. After cooling, the resulting mixture was poured into plenty of stirred water and extracted with chloroform. The obtained organic phase was washed several times with water, dried over magnesium sulfate, evaporated, and purified with column chromatography on silica gel (hexane/acetone, v/v, 8:1) to yield yellowish oil. (4.23 g , 62%).

^{1}H NMR (400 MHz, $CDCl_3$) δ 7.22 (d, *J* = 8.6 Hz, 2H), 6.94 (d, *J* = 8.4 Hz, 4H), 6.65 (d, *J* = 8.3 Hz, 2H), 6.51 (d, *J* = 8.5 Hz,4H), 3.16 (m, 8H), 1.49 (m ,8H), 1.33 – 1.20 (m,8H), 0.88 (t, *J* = 7.3 Hz, 12H).

^{13}C NMR (100 MHz, $CDCl_3$) δ 146.31, 133.59, 132.94, 128.13, 125.22, 115.62, 112.49, 50.96, 29.49, 28.78, 20.39, 13.90.

MALDI-TOF: m/z calcd for $C_{35}H_{48}N_4$: 524.78 $[M]^+$; found: 524.49.

3.2.14 Synthesis of compound 3c

Aproach 1: Under N_2, the mixture of CuI (0.38 g, 0.002 mol), DMPAO (0.76 g, 0.004 mol), aryl 1d (5.27g, 0.01 mol), K_3PO4 (8.49g, 0.04 mol). The tube was evacuated and backfilled with argon, and then dibutylaminee (3.88g, 0.03 mol) and DMSO (40 mL) was added. The reaction mixture was stirred at 100 ℃ for 48 h. After aryl halide was consumed, water was added and the mixture was extracted with ethyl acetate. The organic layer was dried over $MgSO_4$ and evaporated. The residue was purified by column chromatography on silica gel (hexane/acetone, v/v, 50:1). Red oil was obtained (2.26 g, 43%).

Aproach 2: To a solution of 2c (2.63 g, 5 mmol) in dry toluene (30 mL) was added a 1 M solution of diisobutylaluminum hydride in hexanes (10 mL, 10 mmol) by syringe at -78 °C with a dry ice/acetone bath. The reaction was stirred at -78 °C for 2 h. After the mixture was warmed to room temperature, NH_4Cl solution was added to quench the reaction. The mixture was stirred for 1h to complete the hydrolysis. The organic solvent was collected and removed in vacuo. The residue was purified by column chromatography on silica gel (hexane/acetone, v/v, 10/1) to yield red oil (2.19 g, 83%).

^{1}H NMR (400 MHz, $CDCl_3$) δ 9.62 (s, 1H), 7.50 (d, *J* = 8.5 Hz, 2H), 6.96 (d, *J* = 8.5 Hz, 4H), 6.72 (d, *J* = 8.4 Hz, 2H), 6.52 (d, *J* = 8.7 Hz, 4H), 3.22 – 3.11 (m,8H), 1.58 – 1.41 (m, 8H), 1.36 – 1.20 (m, 8H), 0.88 (m, 12H).

^{13}C NMR (100 MHz, $CDCl_3$) δ 190.11, 146.31, 133.73, 131.47, 131.36, 128.57, 128.16, 126.47, 125.82, 124.59, 117.42, 115.33, 112.40, 50.80, 29.48, 20.38, 14.02.

MALDI-TOF: m/z calcd for $C_{35}H_{49}N_3O$:527.78 $[M]^+$; found: 527.79.

3.2.15 Synthesis of compound 4c

In a similar manner described above, compound 4c was synthesized from 3c as a red liquid (67%).

^{1}H NMR (400 MHz, Acetone) δ 7.17-7.12 (m,3H),7.00 (m, 2H), 6.92 (d, *J* = 3.1 Hz, 2H), 6.88 – 6.84 (m, 2H), 6.82 – 6.78 (m, 1H), 6.55 (m, 6H), 6.43 (d, *J* = 11.6 Hz, 1H), 3.18 (m, 8H), 1.51 – 1.37 (m, 8H), 1.24 (m, 8H), 0.82 (m, 12H).

^{13}C NMR (100 MHz, Acetone) δ 146.36, 144.62, 141.21, 130.33, 130.13, 128.53, 128.40, 127.37, 125.87, 124.15, 121.50, 118.96, 118.11, 113.60, 51.57, 20.99, 14.39.

MALDI-TOF: m/z calcd for $C_{40}H_{53}N_3S$: 607.93 $[M]^+$; found: 607.76.

3.2.16 Synthesis of compound 5c

In a similar manner described above, compound 4b was synthesized from 3b as a red liquid (84%).

^{1}H NMR (400 MHz, Acetone) δ 9.78 (s, 1H), 7.69 (d, *J* = 3.8 Hz, 1H), 7.15 (d, *J* = 3.8 Hz, 1H), 7.08 -6.94 (m, 6H), 6.71 – 6.49 (m, 8H), 3.59 – 2.88 (m, 8H), 1.58 – 1.42 (m, 8H), 1.30 (m, 8H), 0.86 (m, 12H).

^{13}C NMR (100 MHz, $CDCl_3$) δ 188.05, 154.88, 150.79, 147.37, 141.92, 139.10, 134.15, 132.93, 117.84, 25.28, 18.70.

MALDI-TOF: m/z calcd for $C_{41}H_{53}N_3OS$: 635.94 $[M]^+$; found: 635.96.

3.2.17 Synthesis of chromophore T3

In a similar manner described above, chromophore T3 was synthesized from 4b and acceptor 5, as a dark solid (40%).

^{1}H NMR (400 MHz, Acetone) δ 8.15 (d, J = 15.8 Hz, 1H), 7.67 (d, J = 3.8 Hz, 1H), 7.41 (d, J = 8.4 Hz, 2H), 7.23 (m, 3H), 7.03 (d, J = 8.5 Hz, 4H), 6.82 (d, J = 15.9 Hz, 1H), 6.72 (dd, J = 16.0, 8.6 Hz, 6H), 3.37 – 3.26 (m, 8H), 1.87 (d, J = 14.6 Hz, 6H), 1.65 – 1.51 (m, 8H), 1.46 – 1.28 (m, 10H), 0.96 (t, J = 7.3 Hz, 11H).

^{13}C NMR (100 MHz, Acetone) δ 176.45, 174.21, 153.17, 150.82, 145.82, 139.66, 138.01, 137.87, 134.75, 133.71, 130.51, 128.45, 128.04, 127.76, 127.47, 125.85, 116.76, 116.68, 112.57, 112.36, 111.73, 110.85, 98.11, 97.22, 54.37, 50.59, 25.37, 20.03, 13.34.

MALDI-TOF: m/z calcd for $C_{52}H_{60}N_6OS$: 817.14 $[M]^+$; found: 817.26.

Anal. calcd (%) for $C_{52}H_{60}N_6OS$: C, 76.43; H, 7.40; N, 10.28; found: C, 76.54; H, 7.36; N, 10.33.

4. Conclusion

In this research, a series of NLO chromophores based on modified TAA donor have been synthesized and systematically investigated by NMR, MS and UV-vis absorption spectra. The energy gap between ground state and excited state together with molecular nonlinearity were studied by UV-vis absorption

spectroscopy, DFT calculations and CV measurements. Theoretical and experimental investigations suggest that introducing the heteroatom to the benzene ring of TAA donor can dramatically affect their nonlinear optical properties. The poling results of guest-host EO polymers with 25 wt% of these chromophores showed that polymers with chromophores T1-T3 afforded the large r_{33} values of 16, 58 and 95 pm/V respectively. The derived chromophores exhibit good thermal stability and large molecular hyperpolarizabilities, which can be effectively translated into very large electro-optic coefficients in poled polymers. We believe that these new chromophores can be used in exploring high-performance organic EO and photorefractive materials where both thermal stability and optical nonlinearity are of equal importance**.**

5. Acknowledgements

We are grateful to the National Nature Science Foundation of China (no. 61101054) for financial support.

Notes and references

a Key Laboratory of Photochemical Conversion and Optoelectronic Materials, Technical Institute of Physics and Chemistry, Chinese Academy of Sciences, Beijing 100190, PR China

b University of Chinese Academy of Sciences, Beijing 100043, PR China

** Corresponding authors. Tel.: +86-01-82543528; Fax: +86-01-62554670.*

E-mail address: xinhouliu@foxmail.com and xhliu@mail.ipc.ac.cn (X. Liu)

1. H. C. Song, M. C. Oh, S. W. Ahn, W. H. Steier, H. R. Fetterman and C. Zhang, *Appl. Phys. Lett.*, 2003, **82**, 4432-4434.
2. L. Dalton, *Polymers for Photonics Applications I*, 2002, **158**, 1-86.
3. A. M. Sinyukov, M. R. Leahy, L. M. Hayden, M. Haller, J. D. Luo, A. K. Y. Jen and L. R. Dalton, *Appl. Phys. Lett.*, 2004, **85**, 5827-5829.
4. J. A. Davies, A. Elangovan, P. A. Sullivan, B. C. Olbricht, D. H. Bale, T. R. Ewy, C. M. Isborn, B. E. Eichinger, B. H. Robinson, P. J. Reid, X. Li and L. R. Dalton, *J. Am. Chem. Soc.*, 2008, **130**, 10565-10575.
5. J. Luo, Y.-J. Cheng, T.-D. Kim, S. Hau, S.-H. Jang, Z. Shi, X.-H. Zhou and A. K. Y. Jen, *Org. Lett.*, 2006, **8**, 1387-1390.
6. M. J. Cho, S. K. Lee, J. I. Jin, D. H. Choi and L. R. Dalton, *Thin Solid Films*, 2006, **515**, 2303-2309.
7. L. Wang, J. L. Liu, S. H. Bo, Z. Zhen and X. H. Liu, *Mater. Lett.*, 2012, **80**, 84-86.
8. J. Wu, J. Liu, T. Zhou, S. Bo, L. Qiu, Z. Zhen and X. Liu, *RSC Advances*, 2012, **2**, 1416.
9. P. A. Sullivan, H. Rommel, Y. Liao, B. C. Olbricht, A. J. P. Akelaitis, K. A. Firestone, J.-W. Kang, J. Luo, J. A. Davies, D. H. Choi, B. E. Eichinger, P. J. Reid, A. Chen, A. K. Y. Jen, B. H. Robinson and L. R. Dalton, *J. Am. Chem. Soc.*, 2007, **129**, 7523-7530.
10. M. Q. He, T. M. Leslie, J. A. Sinicropi, S. M. Garner and L. D. Reed, *Chem. Mater.*, 2002, **14**, 4669-4675.
11. L. Dalton and S. Benight, *Polymers*, 2011, **3**, 1325-1351.
12. P. A. Sullivan, A. J. P. Akelaitis, S. K. Lee, G. McGrew, S. K. Lee, D. H. Choi and L. R. Dalton, *Chem. Mater.*, 2006, **18**, 344-351.
13. S. R. Marder, C. B. Gorman, F. Meyers, J. W. Perry, G. Bourhill, J. L. Bredas and B. M. Pierce, *Science*, 1994, **265**, 632-635.
14. Yi Liao, †, Bruce E. Eichinger, †, Kimberly A. Firestone, †, Marnie Haller, ‡, Jingdong Luo, ‡, Werner Kaminsky, †, Jason B. Benedict, †, Philip J. Reid, †, Alex K-Y Jen and †, *J. AM. CHEM. SOC. 2005, 127, 2758-2766*, 2005, **127**, 2758-2766.
15. S. R. Hammond, O. Clot, K. A. Firestone, D. H. Bale, D. Lao, M. Haller, G. D. Phelan, B. Carlson, A. K. Y. Jen, P. J. Reid and L. R. Dalton, *Chem. Mater.*, 2008, **20**, 3425-3434.
16. J. Wu, S. Bo, J. Liu, T. Zhou, H. Xiao, L. Qiu, Z. Zhen and X. Liu, *Chem Commun (Camb)*, 2012, **48**, 9637-9639.
17. P. Si, J. Liu, Z. Zhen, X. Liu, G. Lakshminarayana and I. V. Kityk, *Tetrahedron Lett.*, 2012, **53**, 3393-3396.
18. J. D. Luo, M. Haller, H. Ma, S. Liu, T. D. Kim, Y. Q. Tian, B. Q. Chen, S. H. Jang, L. R. Dalton and A. K. Y. Jen, *J. Phys. Chem. B*, 2004, **108**, 8523-8530.
19. S. Liu, M. A. Haller, H. Ma, L. R. Dalton, S. H. Jang and A. K. Y. Jen, *Adv. Mater.*, 2003, **15**, 603-607.
20. Y. J. Cheng, J. D. Luo, S. Hau, D. H. Bale, T. D. Kim, Z. W. Shi, D. B. Lao, N. M. Tucker, Y. Q. Tian, L. R. Dalton, P. J. Reid and A. K. Y. Jen, *Chem. Mater.*, 2007, **19**, 1154-1163.
21. S. M. Budy, S. Suresh, B. K. Spraul and D. W. Smith, Jr., *Journal of Physical Chemistry C*, 2008, **112**, 8099-8104.
22. S. Suresh, H. Zengin, B. K. Spraul, T. Sassa, T. Wada and D. W. Smith, *Tetrahedron Lett.*, 2005, **46**, 3913-3916.
23. C. Z. Cai, I. Liakatas, M. S. Wong, M. Bosch, C. Bosshard, P. Gunter, S. Concilio, N. Tirelli and U. W. Suter, *Org. Lett.*, 1999, **1**, 1847-1849.
24. Y. Yang, H. Xu, F. Liu, H. Wang, G. Deng, P. Si, H. Huang, S. Bo, J. Liu, L. Qiu, Z. Zhen and X. Liu, *Journal of Materials Chemistry C*, 2014, **2**, 5124-5132.
25. H. Ma, B. Chen, T. Sassa, L. R. Dalton and A. K. Y. Jen, *J. Am. Chem. Soc.*, 2001, **123**, 986-987.
26. H. Ma, S. Liu, J. D. Luo, S. Suresh, L. Liu, S. H. Kang, M. Haller, T. Sassa, L. R. Dalton and A. K. Y. Jen, *Adv. Funct. Mater.*, 2002, **12**, 565-574.
27. C. W. Tang and S. A. Vanslyke, *Appl. Phys. Lett.*, 1987, **51**, 913-915.
28. M. F. Semmelhack, P. Helquist, L. D. Jones, L. Keller, L. Mendelson, L. S. Ryono, J. G. Smith and R. D. Stauffer, *J. Am. Chem. Soc.*, 1981, **103**, 6460-6471.
29. H. C. Li, Y. H. Geng, S. W. Tong, H. Tong, R. Hua, G. P. Su, L. X. Wang, X. B. Jing and F. S. Wang, *Journal of Polymer Science Part a-Polymer Chemistry*, 2001, **39**, 3278-3286.
30. R. M. Dickson and A. D. Becke, *J. Chem. Phys.*, 1993, **99**, 3898-3905.
31. M. Frisch, G. Trucks, H. Schlegel, G. Scuseria, M. Robb, J. Cheeseman, J. Montgomery Jr, T. Vreven, K. Kudin and J. Burant, *Gaussian Inc., Pittsburgh, PA*, 2003.
32. C. Lee and R. G. Parr, *Physical Review A*, 1990, **42**, 193-200.
33. X. Ma, F. Ma, Z. Zhao, N. Song and J. Zhang, *J. Mater. Chem.*, 2010, **20**, 2369.
34. R. V. Solomon, P. Veerapandian, S. A. Vedha and P. Venuvanalingam, *J. Phys. Chem. A*, 2012, **116**, 4667-4677.
35. R. M. El-Shishtawy, F. Borbone, Z. M. Al-Amshany, A. Tuzi, A. Barsella, A. M. Asiri and A. Roviello, *Dyes and Pigments*, 2013, **96**, 45-51.
36. J. Y. Wu, J. L. Liu, T. T. Zhou, S. H. Bo, L. Qiu, Z. Zhen and X. H. Liu, *Rsc Advances*, 2012, **2**, 1416-1423.

37. K. S. Thanthiriwatte and K. M. N. de Silva, *Journal of Molecular Structure-Theochem*, 2002, **617**, 169-175.
38. C. C. Teng and H. T. Man, *Appl. Phys. Lett.*, 1990, **56**, 1734.
39. L. R. Dalton, D. Lao, B. C. Olbricht, S. Benight, D. H. Bale, J. A. Davies, T. Ewy, S. R. Hammond and P. A. Sullivan, *Opt. Mater.*, 2010, **32**, 658-668.
40. W. B. Wu, J. G. Qin and Z. Li, *Polymer*, 2013, **54**, 4351-4382.
41. M. Q. He, T. M. Leslie and J. A. Sinicropi, *Chem. Mater.*, 2002, **14**, 2393-2400.
42. Z. Ning, Z. Chen, Q. Zhang, Y. Yan, S. Qian, Y. Cao and H. Tian, *Adv. Funct. Mater.*, 2007, **17**, 3799-3807.

Graphical abstract

Introduing the heteroatom to the TAA donor can efficiently improve the electron-donating ability and enhance EO activity.